Hydrodynamic theory for ion structure and stopping power in quantum plasmas

P. K. Shukla[1,2,3,4,*] and M. Akbari-Moghanjoughi[5,6]

[1]*International Centre for Advanced Studies in Physical Sciences & Institute for Theoretical Physics, Faculty of Physics & Astronomy, Ruhr University Bochum, D-44780 Bochum, Germany and Research Department Plasmas with Complex Interactions, Ruhr University Bochum, D-44780 Bochum, Germany*

[2]*Department of Mechanical and Aerospace Engineering & Center for Energy Research, University of California San Diego, La Jolla, California 92093, USA*

[3]*Scottish Universities Physics Alliance, Department of Physics, University of Strathclyde, Glasgow G4 ONG, United Kingdom*

[4]*School of Chemistry and Physics, University of Kwazulu-Natal, Durban 4000, South Africa*

[5]*Azarbaijan Shahid Madani University, Faculty of Sciences, Department of Physics, 51745-406 Tabriz, Iran*

[6]*International Centre for Advanced Studies in Physical Sciences & Institute for Theoretical Physics, Ruhr University Bochum, D-44780 Bochum, Germany*

(Received 2 January 2013; revised manuscript received 7 March 2013; published 12 April 2013)

We present a theory for the dynamical ion structure factor (DISF) and ion stopping power in an unmagnetized collisional quantum plasma with degenerate electron fluids and nondegenerate strongly correlated ion fluids. Our theory is based on the fluctuation dissipation theorem and the quantum plasma dielectric constant that is deduced from a linearized viscoelastic quantum hydrodynamical (LVQHD) model. The latter incorporates the essential physics of quantum forces, which are associated with the quantum statistical pressure, electron-exchange, and electron-correlation effects, the quantum electron recoil effect caused by the dispersion of overlapping electron wave functions that control the dynamics of degenerate electron fluids, and the viscoelastic properties of strongly correlated ion fluids. Both degenerate electrons and nondegenerate strongly correlated ions are coupled with each other via the space charge electric force. Thus, our LVQHD theory is valid for a collisional quantum plasma at atomic scales with a wide range of the ion coupling parameter, the plasma composition, and plasma number densities that are relevant for compressed plasmas in laboratories (inertial confinement fusion schemes) and in astrophysical environments (e.g., warm dense matter and the cores of white dwarf stars). It is found that quantum electron effects and viscoelastic properties of strongly correlated ions significantly affect the features of the DISF and the ion stopping power (ISP). Unlike previous theories, which have studied ion correlations in terms of the ion coupling parameter, by neglecting the essential physics of collective effects that are competing among each other, we have here developed a method to evaluate the dependence of the plasma static and dynamical features in terms of individual parameters, like the Wigner-Seitz radius, the ion atomic number, and the ion temperature. It is found that due to the complex nature of charge screening in quantum plasmas, the ion coupling parameter alone cannot be a good measure for determining ion correlation effects in a collisional quantum plasma, and such a characteristic of a dense quantum plasma should be evaluated against each of the plasma parameters involved. The present investigation thus provides testable predictions for the DISF and ISP and is henceforth applicable to a wide range of compressed plasma categories ranging from laboratory to astrophysical warm dense matter.

DOI: 10.1103/PhysRevE.87.043106 PACS number(s): 52.30.−q, 71.10.Ca, 05.30.−d

I. INTRODUCTION

Study of collective effects in strongly coupled nonideal plasmas [1–6] is of great importance in almost all branches of plasma physics research, ranging from the plasma diagnostics by lasers and intense laser-matter interactions [7], dusty plasmas with strongly correlated highly charged dust grains [8], as well as laboratory and astrophysical warm dense matter (WDM) [9]. A fundamental issue of the plasma diagnostics in high-energy-density plasma physics research is an accurate determination of the plasma parameters, such as the electron number density and the ambient plasma temperature. Many important properties of dense plasmas are the electrical and thermal conductivities, optical properties, ionization, dielectric polarization, electronic density correlation, and fusion cross section. Those properties are strongly affected by the ion and electron coupling parameters, which are denoted by $\Gamma_i = Z_i^2 e^2/r_0 k_B T_i$ and $\Gamma_e = e^2/r_0 k_B T_e$, respectively, where Z_i is the ion charge state, e the magnitude of the electron charge, $r_0 = (3/4\pi n_{i,e})^{1/3}$ the average interelectron spacing or the Wigner-Seitz (WS) radius, k_B the Boltzmann constant, and T_i (T_e) the ion (electron) temperature. Strong ion couplings in a dense plasma can coexist with quantum mechanical effects associated with electron degeneracy [10–12]. The latter comes into the picture [13] when the electron thermal de Broglie wavelength, $\Lambda_D = \hbar/m_e V_T$, is comparable with r_0, where $\hbar$ is Planck's constant divided by 2π, m_e the electron rest mass, $V_T = \sqrt{k_B T_p/m_e}$ the thermal speed of electrons due to their random motion, and T_p the plasma temperature. Also, in a dense quantum plasma, λ_D is much smaller than the Landau length $\lambda_L = e^2/k_B T_p$. Furthermore, in characterizing a dense quantum plasma the degeneracy parameter $\Theta_d = T_{Fe}/T_p$, where T_{Fe} is the electron Fermi temperature, also plays an important role in determining the strength of the quantum electron interactions.

In a quantum plasma with $\Theta_d < 1$ degenerate electrons form quantum electron fluids, while nondegenerate ions behave like viscoelsatic charged fluids due to their much

*Deceased.

smaller kinetic energy in comparison with that of the electrons. On the other hand, in dense plasmas with $\Gamma_i > 1$ the ions are strongly correlated due to their lower thermal kinetic energy, while degenerate electrons are mildly correlated because they have relatively higher kinetic energy. However, ion degeneracy and electron couplings could become important in extremely cold dense matter, such as neutron stars [14], where the electron number density typically exceeds 10^{35} cm^{-3} and the plasma particle temperature is below 10^4 K. The plasma regime with $\Theta_d \simeq \Gamma_i \simeq 1$ is usually referred to as WDM. Simulations have revealed that for a wide range of the plasma number densities beyond solid density and the ion temperature regimes with $1 < \Gamma_i < 176$, the plasma state is in liquid phase with strongly correlated ions [15].

It is well known that the study of the structural properties of alkali and alkaline earth plasmas, such as lithium and beryllium, is of fundamental importance in high-energy-density technologies. The ionic structure factor is a fundamental property of the plasma x-ray scattering cross section. Pulsed-power-driven high-energy-density (PPD-HED), Z-pinches, and inertial confinement fusion (ICF) techniques, therefore, strongly rely on the basic knowledge of the ion structure factor of matter in extreme conditions, such as high temperature and densities. The static and dynamic structure factor for high-temperature alkali and alkaline earth plasma has been extensively studied in Ref. [16], using direct numerical simulation methods based on the moment approach. On the other hand, the study of the plasma state via the dynamical ion structure factor (DISF) is also of fundamental importance in compact astrophysical environments [17–19] and in WDM [20,21]. For instance, information on structures of the cores of giant planets like Jupiter [22–25] and compact stars like white dwarfs may provide answers to a long sought question on the evolution of stellar chains and phase transitions in extremely dense hot matter [26]. It is also instructive to investigate the effect of relativistic electron degeneracy, originally established by Hoyle and Fowler [11], on strong couplings and ion structures in dense quantum plasmas. The relativistic electron degeneracy can lead to a distinct equation of state of matter and the well-known Chandrasekhar mass limit [10]. It has also been shown that the important interacting potentials, such as the Coulomb and electron-exchange interactions, can lead to significant corrections to the Chandrasekhar mass limit [27] for white dwarf stars. In the past, based on the spectral analysis of lithium, beryllium and graphite, Priftis *et al.* [28] reported the first evidence for the plasmon scattering besides the usual Compton and Rayleigh scattering. Recently, the importance of quantum effects has been demonstrated by scattering of light off electron plasma oscillations in WDM [29] created by compressing plasma to near solid density by intense laser beams [30]. This may be an indication of strong coupling effects in WDM and in strongly coupled quantum plasmas [31].

On the other hand, high-energy x-ray light sources or laser pulsed power technologies have opened new windows for investigating many collective processes [32–44], including ion structure factors (ISFs) in strongly coupled plasma systems [45–48]. The pair correlations in a metallic density regime for a quantum electron fluid has been previously investigated using the random phase approximation (RPA), including the Coulomb and electron exchange effects. It has been remarked that the RPA method provides good description of the plasmon excitation mode only for the long-wavelength screening phenomena, with its validity being limited to high electron densities. The ineffectiveness of the RPA method becomes evident from the fact that the pair-distribution function for small separation between particles (higher electron densities) becomes negative over the entire range of metallic densities [49]. More recently, Shukla and Eliasson [43,50] have shown that in quantum plasmas there appears to be a short-range attractive force between ions due to local electron condensation arising from the constructive interference of electron wave functions on account of the quantum electron recoil effect [38,39]. The short-range Shukla-Eliasson attractive force [43,50], which is associated with a negative electric potential distribution in the electron density regime surpassing solid density and extending up to 10^{26} cm^{-3} [43,50], is capable of bringing ions closer and responsible for the formation of ion clusters. Such an effect, which is found to be present for plasmas with densities even few times below that of solid density, may provide a new ignition criteria for the fast ignition scheme in future inertial confinement fusion devices. Initial molecular dynamics (MD) simulations have revealed ion clustering under such interactions [51]. The ionic structure of one-component plasma (OCP) and Yukawa systems have been extensively studied using computational techniques based on classical Monte Carlo (MC), MD, and density functional theory (DFT). However, the study of quantum plasmas with strong ion couplings requires a detailed theoretical analysis, since the standard investigations usually do not account for important collective interactions. Such interaction may occur between an ensemble of degenerate electrons, strong correlations between nondegenerate ions, and Coulomb collisions among electrons and ions. The best way to make progress is to use the quantum hydrodynamical model for degenerate electrons and a viscoelastic fluid model for strongly correlated ions in a strongly coupled viscous quantum plasma [52]. Recently Mithen *et al.* [53] have investigated the extent of validity of the hydrodynamic description for ISFs in a dense plasma and have concluded that such an approach can be used to effectively model the ion dynamics in a dense plasmas over a wide range of the plasma number densities that can be experimentally probed.

In this paper we present a linear theory for DISF and ISP in a collisional quantum plasma by using the dielectric constant, which is deduced from a set of hydrodynamic equations composed of the continuity, momentum, and Poisson equations. In our model nonrelativistic electron momentum transfer equation includes the electron inertial force and the electric and quantum forces, as well as electron-ion momentum transfer due to collisions, while the ion momentum transfer equation captures the essential physics of the ion correlation decay rate, the ion-electron momentum transfer due to collisions, the shear and bulk ion fluid viscosities, the electrostatic force, and the ion pressure gradient. The fluctuation dissipation theorem in association with the present dielectric constant for a dissipative quantum plasma provides a complete understanding of spectral features of ion plasma oscillations via the DISF and ISP in compressed plasmas that are relevant for inertial confinement fusion (ICF) and astrophysical environments.

The manuscript is organized in the following fashion. In Sec. II we present the governing viscoelastic quantum hydrodynamic (VQHD) equations for our unmagnetized quantum plasma and derive the dielectric constant for electrostatic perturbations. Here we also numerically investigate the properties of the real and imaginary parts of the dielectric constant and highlight the role of the quantum forces (especially the quantum recoil effect) and dissipative forces (*viz.,* electron-ion collisions) that are essential for depicting the new spectral features of the ion plasma oscillations. The latter are responsible for bringing new aspects of the DISF and ISP in a dense quantum plasma. Section III contains a detailed investigation of the dynamic and static ion structure factors. Analytical and numerical results for the ISP are presented in Sec. IV. A brief summary and conclusions are given in Sec. V.

II. THE GOVERNING EQUATIONS AND THE DIELECTRIC CONSTANT

In this section we present our VQHD equations and use them to obtain the dielectric constant of an unmagnetized quantum plasma. The properties of the dielectric constant are analyzed numerically.

A. The governing VQHD equations

We consider a collisional quantum plasma composed of degenerate electron fluids and strongly correlated nondegenerate ion fluids. The strength of the ion coupling parameter is defined by $\Gamma_i = \langle U_{\rm pot}\rangle/\langle U_{\rm kin}\rangle$, where $\langle U_{\rm pot}\rangle$ and $\langle U_{\rm kin}\rangle$ are the average potential and kinetic energies of the ions that are shielded by degenerate electrons, respectively. It should be noted that for a quantum plasma to be in a condensed matter state the ion coupling parameter can be as high as 170 [15]. The governing VQHD equations, including all significant plasma interaction energies, such as the Coulomb, the quantum electron pressure degeneracy, the quantum electron recoil, electron-exchange, and electron correlations, is composed of the continuity, momentum, and Poisson equations [41]:

$$\begin{aligned}
&\frac{dn_{i,e}}{dt} + n_{i,e}\nabla\cdot\mathbf{u}_{i,e} = 0,\\
&\frac{d}{dt} = \frac{\partial}{\partial t} + \mathbf{u}\cdot\nabla,\\
&\left(1+\tau_i\frac{d}{dt}\right)\left[m_i n_i\frac{d\mathbf{u}_i}{dt} + Z_i e n_i\nabla\phi - \nabla P_i\right.\\
&\qquad\left. + Z_i n_i m_i \nu_{ie}(u_i - u_e)\right]\\
&\quad = \eta_i[\nabla^2\mathbf{u}_i + (\xi_i + \eta_i/3)\nabla(\nabla\cdot\mathbf{u}_i)],\\
&m_e\left(\frac{d}{dt} + \nu_{ei}\right)\mathbf{u}_e - m_e\nu_{ei}u_i\\
&\quad = e\nabla\phi - \frac{1}{n_e}\nabla P_G + \frac{\hbar^2\nabla}{2m_e}\left(\frac{\Delta\sqrt{n_e}}{\sqrt{n_e}}\right),\\
&\nabla^2\phi = 4\pi e(n_e - Z_i n_i),
\end{aligned} \tag{1}$$

where n_j and $\mathbf{u}_j$ are the number density and the fluid velocity of the particle species j, respectively (j equals e for degenerate electrons and i for nondegenerate ions), ϕ the electrostatic potential, $P_i = \mu_i n_i k_B T_i$ the ion pressure, μ_i the ion fluid compressibility that depends on Γ_i, and m_i, τ_i, $\nu_{ei}(\nu_{ie})$, and $\eta_i(\xi_i)$ are the ion mass, viscoelastic relaxation time for the ion fluid, electron-ion (ion-electron) collision frequency, and ion shear (bulk) viscosity, respectively. We have neglected the electron correlation decay rate and the electron fluid viscosities because degenerate electrons are in a mildly coupled state. We note that the electron fluid viscosity may be significant only at much larger densities relevant to neutron-star crusts [54], which we will ignore in the present analysis. Here we focus on compressed plasmas with densities surpassing solid density and below the core densities of white dwarf stars, which are several orders of magnitude lower than that in neutron star crusts. On the other hand, in our quantum plasma we have $Z_i n_i m_i \nu_{ie} \simeq n_e m_e \nu_{ei}$. Furthermore, under the assumptions $\omega/\omega_{pe,pi} \ll \omega_{pe,pi}/\nu_{ei,ie}$, where $\omega_{pe,pi} = \sqrt{4\pi e^2 n_e/m_{e,i}}$ is the plasma frequency of the species $j = e,i$, the electron and ion fluids become collisionally decoupled. The parameter $P_G = P_{\rm deg} + P_C + P_{xc}$ includes all the dominant electron interaction pressures, a detailed description of which follows.

The generalized quantum electron degeneracy pressure, which incorporates the relativistic electron dynamics and is valid for a much wider range of the electron number density, is given by Chandrasekhar [12]:

$$P_{\rm deg} = \frac{\pi m_e^4 c^5}{3h^3}[R(2R^2-3)\sqrt{1+R^2} + 3\sinh^{-1}R] \tag{2}$$

in which $R = P_{Fe}/m_e c$ is the normalized relativistic Fermi momentum used as a measure for the degree of plasma degeneracy and is related to the plasma number density as $R = (\rho/\rho_c)^{1/3}$ with $\rho_c \simeq 2\times 10^6$ g/cm^3 is the normalizing plasma mass density, and other quantities have their usual meanings. It is observed that $R = \{0,\infty\}$ limits of the Chandrasekhar's generalized pressure correspond to non- and ultrarelativistic degeneracy pressure cases with polytropic indices of $\Gamma_i = \{5/3,4/3\}$, respectively [10]. It has been shown that the plasma dynamics may be significantly altered due to a change in the equation of state [55] of matter by going from non- to ultrarelativistic electron degeneracy regime.

The Salpeter's Coulomb interaction among ions and electrons [27] introduces another important correction to quantum pressure, which is a negative contribution and has been shown to slightly alter the Chandrasekhar's mass-radius relation. The mechanism of such a negative pressure is similar to the cohesive binding present in most ionic lattice. Hence, a quantum electron-ion plasma can act like ionic crystal giving rise to ionic dielectric response, as will be apparent later. This is different from the ordinary electronic (atomic) polarization caused by asymmetric electron distribution around ions. In the spherical and noninteracting Wigner-Seitz approximation, the Coulomb negative pressure can be written as [27]

$$P_C = -\frac{8\pi^3 m_e^4 c^5}{h^3}\left[\frac{\alpha Z_i^{2/3}}{10\pi^2}\left(\frac{4}{9\pi}\right)^{1/3}\right]R^4, \tag{3}$$

where $\alpha = e^2/\hbar c \simeq 1/137$ is the fine structure constant. The electron-exchange pressure as a function of the Chandrasekhar's relativity parameter, R, is given by Salpeter

and Zapolsky [27] as

$$P_{xc} = -\frac{2\alpha m_e^4 c^5}{h^3}\left\{\frac{1}{32}(\beta^4+\beta^{-4})+\frac{1}{4}(\beta^2+\beta^{-2}) - \frac{3}{4}(\beta^2-\beta^{-2})\ln\beta - \frac{9}{16}+\frac{3}{2}(\ln\beta)^2 - \frac{R}{3}\left(1+\frac{R}{\sqrt{1+R^2}}\right)\left[\frac{1}{8}(\beta^3-\beta^{-5})-\frac{1}{4}(\beta-\beta^{-3}) - \frac{3}{2}(\beta+\beta^{-3})\ln\beta+\frac{3\ln\beta}{\beta}\right]\right\}, \quad (4)$$

where $\beta = R+\sqrt{1+R^2}$. It has been shown that the electron exchange energy can play a dominant role in the electron potential screening in quantum plasmas and together with the quantum recoil effect caused by the Bohm force, $F_B = -(\hbar^2\nabla/2m_e)(\Delta\sqrt{n_e}/\sqrt{n_e})$, can lead to the Lennard-Jones-like attractive force between ions of similar charge [41]. The Shukla-Eliasson (SE) attraction is attributed to the electron diffraction effect and the spacial localization of electron density between ions of the same charge, which gives rise to a similar effect as the Coulomb interaction pressure, mentioned earlier, and the corresponding ion dielectric response in quantum plasmas.

We now present the ion viscosity parameters of a quantum plasma. Nandkumar and Pethick [56] have calculated electrical conductivity, $\sigma = n_e e^2/\nu_{ei} m_e^*$ (based on a simple Drude model), and the ion shear viscosity, $\eta_i = n_e P_{Fe}^2 \tau_i/5m_e^*$ ($m_e^* = m_e\sqrt{1+R^2}$ being the relativistic electron mass), of a quantum plasma, using the relativistic electron momentum consideration in terms of Chandrasekhar's well-known relativity parameter. This allows one to study the VQHD theory in a wide range of the plasma number density, excluding the effect of insignificant ξ_i in our quantum plasma. The important parameters for the present analysis, namely, the electron-ion collision frequency ν_{ei}, the ion fluid viscosity η_i, and the corresponding viscoelastic ion relaxation time τ_i, have been estimated by Nandkumar and Pethick [56], based on the Monte Carlo (MC) simulations and analytically expressed in terms of the fitting formulas, given by

$$\eta_i \simeq \frac{\rho_c R_0^5}{Z_i I_2(1+R_0^2)}, \quad \nu_{ei} = \frac{4Z_i e^4 m_e I_1\sqrt{1+R_0^2}}{3\pi\hbar^3},$$
$$I_1 = \sqrt{\frac{\pi}{3}}\ln Z_i^{1/3} + \frac{2}{3}\ln\left(1.3+\frac{2.3}{\sqrt{\Gamma_i}}\right) - \frac{R_0^2}{2+2R_0^2},$$
$$I_2 = \sqrt{\frac{\pi}{3}}\ln Z_i^{1/3} + \frac{2}{3}\ln\left(1.3+\frac{2.3}{\sqrt{\Gamma_i}}\right) - \frac{1+2R_0^2}{2+2R_0^2} + \frac{0.27R_0^2}{1+R_0^2}, \quad (5)$$

where $R_0 = (\rho_0/\rho_c)^{1/3}$ is the relativistic degeneracy parameter with $\rho_0 = m_i n_0$ being the average plasma mass density, and $R = R_0(\rho/\rho_0)^{1/3}$ is the plasma relativity parameter. The ion coupling parameter can also be written in terms of the relativity parameter as $\Gamma_i = 22.75\times10^6 Z_i^{5/3} R_0/T_i$. The value of the ion coupling parameter below $\Gamma_i = 178$ corresponds to the liquid state [15]. Therefore, a hydrogen white dwarf star with the overall density $\rho = 10^6$ g/cm^3 and the ion temperature $T_i = 10^6$ K, despite the extreme mass density, would be in a liquid state. At this stage, we introduce an effective potential based on the generalized pressure, which makes the calculations much easier. The corresponding effective potential can be calculated as

$$\Psi_G = \frac{1}{c^2}\int\frac{d_R P_G(R)}{n}dR = \sqrt{1+R^2} - \zeta R + \frac{\alpha}{2\pi}\left(R - \frac{3\sinh^{-1}R}{\sqrt{1+R^2}}\right), \quad (6)$$

where $\zeta = 3^{1/3}(2\alpha/5)(2Z_i/\pi)^{2/3}$.

B. The plasma dielectric constant

In this section we obtain the dielectric constant for our quantum plasma by linearizing the VQHD equations. Accordingly, we let $n_j = n_0 + n_{j1}$, where $n_{j1} \ll n_0$, and suppose that n_{j1} and ϕ are proportional to $\exp[-i(\omega t - \mathbf{k}\cdot\mathbf{r})]$, where ω and $\mathbf{k}$ are the angular frequency and the wave vector of the electrostatic disturbances. Thus, letting $\partial/\partial t = -i\omega$ and $\nabla = i\mathbf{k}$ in Eqs. (1)–(4) and manipulating the resultant equations, we obtain the dielectric constant $\varepsilon(\omega,\mathbf{k}) = 1+\chi_e(\omega,\mathbf{k})+\chi_i(\omega,\mathbf{k})$, where $\chi_e(\omega,\mathbf{k})$ and $\chi_i(\omega,\mathbf{k})$ are the dielectric susceptibility of the electron and ion fluids, respectively. The dimensionless susceptibilities for the electron and ion fluids are, respectively,

$$\chi_e(\omega,\mathbf{k}) \approx [u_B^4 k^4 + u_Q^2 k^2 - \omega^2 - i\nu\omega]^{-1},$$
$$\chi_i(\omega,\mathbf{k}) \approx \left\{\frac{2i\eta k^2}{3(1-i\tau\omega)R_0^3} - \mu\omega^2\right\}^{-1}, \quad (7)$$

where the angular frequency ω and the wave vector $\mathbf{k}$ are in units of the ion plasma frequency $\omega_{pi} = (4\pi Z_i^2 n_0 e^2/m_i)^{1/2}$ and $2\pi/r_B$, respectively. Here $r_B = \hbar^2/m_e e^2$ is the Bohr radius of an hydrogen atom and $\mu = m_i/m_e$. In deducing Eq. (7) we have assumed that the phase velocity of the electrostatic oscillations is much larger than the ion thermal speed $(\mu_i k_B T_i/m_i)^{1/2}$, and the wave frequencies are much smaller that ω_{pe}^2/ν_{ei} and ω_{pi}^2/ν_{ie}. Other parameters are denoted as

$$u_Q^2 = \gamma^2\left\{\frac{R_0^2}{3\sqrt{1+R_0^2}} - \frac{\zeta R_0}{3} + \frac{\alpha}{2\pi}\left[\frac{R_0}{3} - \frac{R_0}{1+R_0^2} + \frac{R_0^2\sinh^{-1}R_0}{(1+R_0^2)^{3/2}}\right]\right\},$$
$$u_B^4 = \gamma^4 H^2, \quad (8)$$

where $\gamma = c/(r_B\omega_{pe})$ and $H = \hbar\omega_{pe}/(2m_e c^2)$ is the dimensionless quantum diffraction parameter. We note that in the above definitions we have used the scaled ion fluid viscosity, as well as the corresponding ion relaxation time and the electron-ion collision parameter is

$$\nu = \frac{\nu_{ei}}{\omega_{pe}} = \frac{1.75\times10^{16}}{\omega_{pe}} Z_i I_1\sqrt{1+R_0^2},$$
$$\tau = \tau_i\omega_{pe} = \frac{2\times10^{-17}\omega_{pe}}{Z_i I_2\sqrt{1+R_0^2}}, \quad \eta = \frac{\gamma\eta_i}{\rho_c} = \frac{\gamma R_0^3}{Z_i I_2(1+R_0^2)}. \quad (9)$$

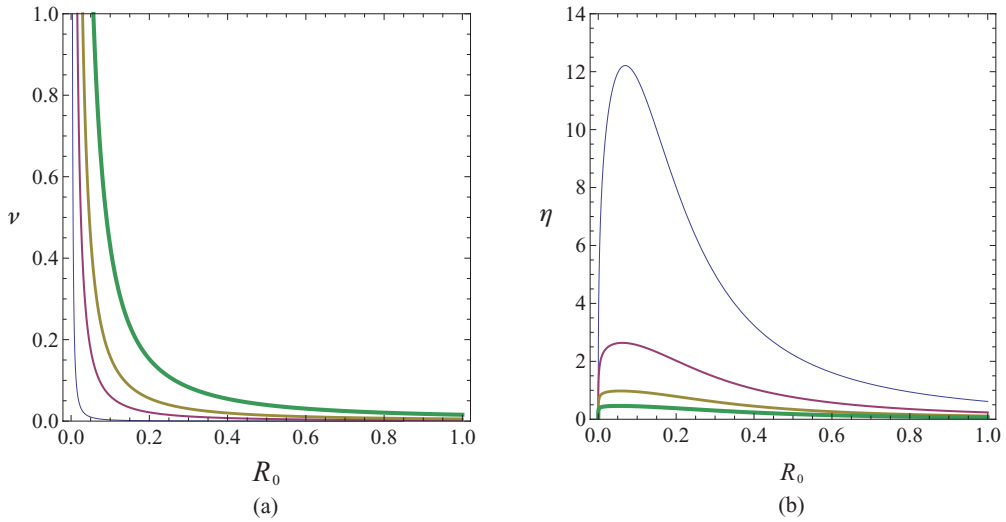

FIG. 1. (Color online) Variation of viscosity, η and electron-ion collision parameters, ν with respect to the relativistic degeneracy parameter, R_0, for different plasma composition, i.e., for (a) $Z_i = 1,6,12,26$ and (b) $Z_i = 3,4,5,6$ and $T_i = 10^4$ K for both plots. The thickness of curves is used as a criterion for an increase in the varied parameter.

In Fig. 1 we display the variations of the normalized electron-ion collision frequency, ν, and normalized viscosity parameter, η, in terms of the relativistic degeneracy parameter, R_0, for different plasma compositions. It is noted that with increase in the relativistic degeneracy parameter, R_0 (or the plasma number density), the electron-ion collision frequency decreases sharply, while the ion fluid viscosity increases, first giving rise to a maximum value in extreme nonrelativistic degenerate density regime, $R_0 < 0.1$, relevant for Jupiter-like planet cores and a WDM scheme, and finally reaches its lowest values for the relativistic density regime, $R_0 > 1$, corresponding to density of typical white dwarfs. On the other hand, the increase in the ion atomic number values is found to cause an increase in the electron-ion collision frequency, for a given value of the relativistic degeneracy parameter value, R_0, but a sudden decrease in the ion fluid viscosity.

The dielectric constant is an important quantity, which can be used to calculate the spectral features of the electron plasma oscillations, ion structure factors, and ion stopping power in plasmas. The real and imaginary parts of the dielectric constant are correlated via the well-known Kramers-Kronig relations

$$\begin{aligned} \mathrm{Re}[\varepsilon(\mathbf{k},\omega)] &= \frac{1}{\pi} P \int_{-\infty}^{+\infty} \frac{\mathrm{Im}[\varepsilon(\mathbf{k},\omega)]}{\omega' - \omega} d\omega', \\ \mathrm{Im}[\varepsilon(\mathbf{k},\omega)] &= -\frac{1}{\pi} P \int_{-\infty}^{+\infty} \frac{\mathrm{Re}[\varepsilon(\mathbf{k},\omega)]}{\omega' - \omega} d\omega', \end{aligned} \tag{10}$$

where Re and Im refer to the real and imaginary parts of the dielectric constant, respectively, and P denotes the Cauchy principal value. The plots in Figs. 2 and 3 display the correlated real and imaginary parts of the dielectric constant for nonrelativistic and relativistic degenerate plasma density regimes, indicating a pronounced plasmon excitation resonance (PER), for a given wave number. A comparison of Figs. 2 and 3 for the effect of plasma number density on PER frequency [plots (a) and (b) in each figure] reveals that in both cases an increase in the plasma number density leads to the sharpening and intensifying of the PER peak and causing the shift of the excitation frequency to lower values. However, such an effect is more pronounced in the nonrelativistic degeneracy regime. Concerning the effect of the ion atomic number, one observes that an increase in the ion atomic number, in contrast to the case of the plasma number density variations, leads to a spreading and mitigation of the PER peaks, again shifting its frequency to lower values [e.g., compare plots (c) and (d) in each figure]. This feature is more distinguished in the nonrelativistic degeneracy regime compared to that of the relativistic one. Finally, from Figs. 2 (panels e and f) and 3 (panels e and f) we observe that an increase in the plasma ion temperature leads to a spread and lowering of PER peaks in both regimes, although this is more pronounced in the nonrelativistic case as compared to the relativistic case. It is thus generally concluded that the plasma parameter variation affects the plasma dielectric response more in the nonrelativistic degeneracy regime than in the relativistic one. Much more physical information can be deduced from the complex dielectric function such as the frequency dependent conductivity and optical properties of the plasma under investigation, for a wide range of plasma density and composition. For instance, the plasma dielectric function is related to the frequency dependent plasma conductivity via $\varepsilon(\omega,k) = 1 + 4\pi i\sigma(\omega,k)/\omega$ with $\sigma(\omega) = \sigma_0/(1 - i\omega\tau)$, where $\sigma_0 = n_0 e^2\tau/m_e$ and τ are the Drude DC-conductivity and electron-ion collision time, respectively. Also, the complex index of refraction is related to the dielectric function by $n(\omega) = \sqrt{\varepsilon(\omega)}$. For normal-angle propagation the optical reflectivity, $r(\omega)$, and absorption coefficient, $a(\omega)$, are given as

$$\begin{aligned} r(\omega) &= \frac{[1 - \mathrm{Re}\sqrt{\varepsilon(\omega)}]^2 + \mathrm{Im}\sqrt{\varepsilon(\omega)}}{[1 + \mathrm{Re}\sqrt{\varepsilon(\omega)}]^2 + \mathrm{Im}\sqrt{\varepsilon(\omega)}}, \\ a(\omega) &= \frac{2\omega \mathrm{Im}\sqrt{\varepsilon(\omega)}}{c}. \end{aligned} \tag{11}$$

On the other hand, the absorption coefficient, $a(\omega)$, is related to the skin depth $\delta(\omega) = 2/a(\omega)$ of the plasma. The

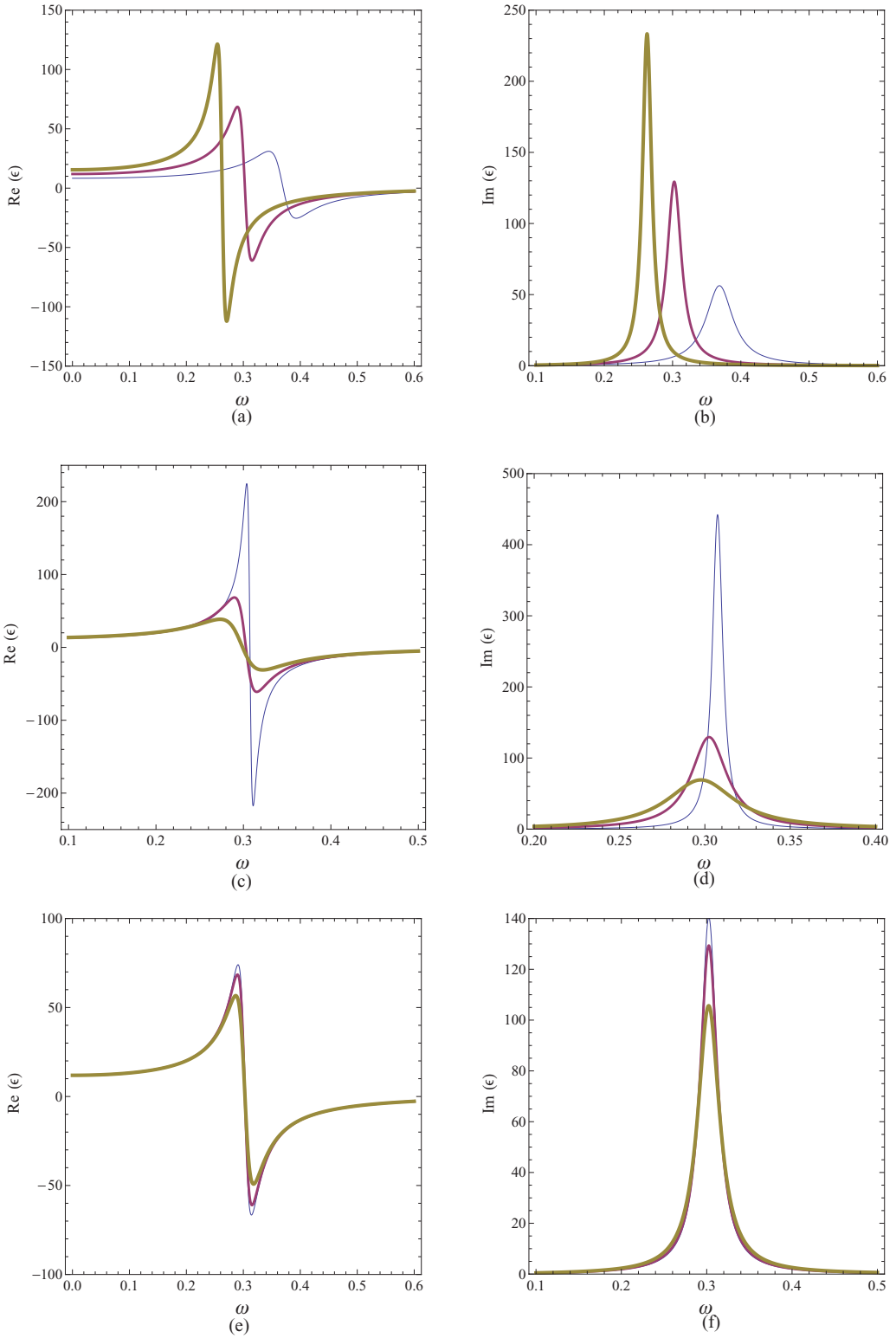

FIG. 2. (Color online) Dielectric linear response (real and imaginary parts) in nonrelativistic degenerate density regime of a viscous collisional quantum plasma for various plasma parameters. The corresponding data used for plots (a) and (b) are $Z_i = 2, n_0 = (3.8, 12.7, 30.2) \times 10^{25}$ cm^{-3}, $k = 1$, $T_i = 10^4$ K, for plots (c) and (d) are $Z_i = 1,2,3$, $n_0 = 12.7 \times 10^{25}$ cm^{-3}, $k = 1$, $T_i = 10^4$ K, and for plots (e) and (f) are $Z_i = 2$, $n_0 = 12.7 \times 10^{25}$ cm^{-3}, $k = 1$, $T_i = (10^3, 10^4, 10^5)$ K. The increase in thickness of curves in each plots indicates the increase in the varied parameter.

frequency-dependent electromagnetic wave attenuation then is given by the well-known relation $I(\omega) = I_0 \exp[-x/\delta(\omega)]$. Comparing Figs. 2 and 3, it becomes evident that the plasma absorption frequency band is much sharper for relativistic degenerate regime compared to that of nonrelativistic one. By close inspection of these figures it is revealed that the

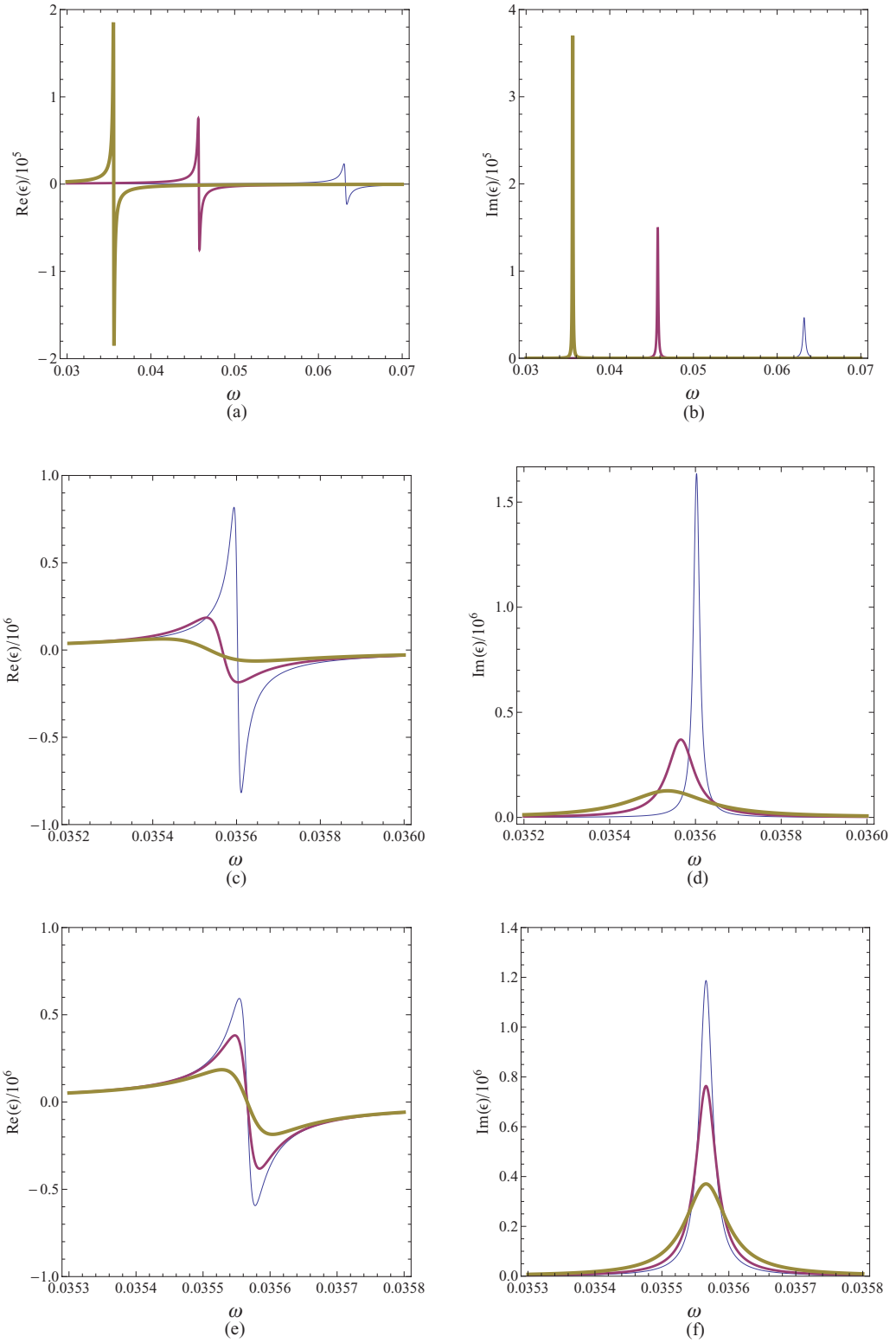

FIG. 3. (Color online) Dielectric linear response (real and imaginary parts) in relativistic degenerate density regime of a viscous collisional quantum plasma for various plasma parameters. The corresponding data used for plots (a) and (b) are $Z_i = 2$, $n_0 = (5.9,47.2,159.3) \times 10^{29}$ cm^{-3}, $k = 1$, $T_i = 10^6$ K, for plots (c) and (d) are $Z_i = 1,2,3$, $n_0 = 47.2 \times 10^{29}$ cm^{-3}, $k = 1$, $T_i = 10^6$ K, and for plots (e) and (f) are $Z_i = 2$, $n_0 = 47.2 \times 10^{29}$ cm^{-3}, $k = 1$, $T_i = (10^4,10^5,10^6)$ K. The increase in thickness of curves in each plot indicates the increase in the varied parameter.

absorption-frequency width decreases by an increase in the plasma number density, while it is broadened by increase in either plasma ion atomic number or its temperature, in both degeneracy regimes. It is worth noting that two distinct frequency limits can be identified for a degenerate electron fluid in the Drude nearly free-electron conductivity model. In

the low-frequency limit, where $\omega\tau \ll 1$, the dielectric function becomes completely imaginary. On the other hand, in the high-frequency limit, $\omega\tau \gg 1$, one can define a plasma edge corresponding to a critical high-frequency limit, (ω_{cr}), below which the plasma exhibits a perfect reflectivity [$r(\omega) = 1$, when we set $\varepsilon(\omega) < 0$ in Eq. (11)]. For $\omega > \omega_{cr}$ we have $\varepsilon(\omega) > 0$, which corresponds to the zero absorption, where $0 < r(\omega) < 1$. It is also noted that the plasma dispersion relation is also obtained by setting; $\mathrm{Re}[\varepsilon(\omega,\mathrm{k})] = 0$. The optical and conductivity plasma parameters are of vital importance, particularly for astrophysical dense plasmas, the detailed calculation of which is out of the scope of the current investigation.

III. THE DYNAMIC AND STATIC ION STRUCTURE FACTORS

Practical information on ion correlations and phase transitions in a dense quantum plasma can be deduced by using our dielectric constant in a detailed calculation of the dynamic ion structure factor (DISF). Figure 4 depicts the variation of the DISF against changes in the plasma parameters. In the present analysis and for small momentum transfer of photons to degenerate electrons, the scattering wave number k is related to the scattering angle θ via $k = 2E_0 \sin\theta/\hbar c$, where E_0 is the incident laser beam energy and c the speed of light in vacuum. The DISF of a plasma with strongly correlated plasma particles represents a description of how strongly correlated electrons or ions scatter an incident electromagnetic radiation against a well-defined frequency spectrum of a plasma system. It is also the quantity describing the inelastic x-ray scattering cross section from a dense plasma or from a simple liquid. The DISF can be directly calculated by using the dielectric constant, via the fluctuation-dissipation theorem, as

$$\frac{S_\omega(k)}{S_0} = k^2 n_B(\omega)\,\mathrm{Im}\left[-\frac{1}{\varepsilon(\omega,k)}\right],$$
$$n_B(\omega) = \frac{1}{1-\exp(-\hbar\omega/\kappa T_i)}. \tag{12}$$

It is noted that the DISF, as given by Eq. (12), contains all the information relevant to both degenerate electron fluids and strongly correlated ion fluids via the dielectric constant $\varepsilon(\omega,\mathbf{k})$. The DISF obeys the relation $S_\omega(k)/S_{-\omega}(-k) = \exp(-\hbar\omega/\kappa T_i)$. The latter predicts an asymmetry in the ion structure factor with respect to ω and k, which usually can be observed in experiments. The asymmetry in the DISF is a common feature (reported by MD simulations) clearly observed in Fig. 5 and due to the existence of inelastic (Compton) and elastic (Rayleigh) scattering of light [21] off tightly or weakly bound electrons, respectively, since the DISF is directly related to spectrally resolved Thomson scattering light signal via the cross-sectional relation, $d^2\delta/d\Omega d\omega = A\delta_T S_\omega(k)$, where $\delta_T \simeq 0.665 \times 10^{-24}$ cm^2 is the usual Thomson cross section and A is a normalizing constant. It is observed from Figs. 5(a) and 5(b) that such an asymmetry is reduced by an increase in the ion temperature. The variation of the asymmetric plasma response in the x-ray regime with respect to the plasma parameter change is shown in Figs. 5(c) and 5(d). It is found that the variation of these parameters has only a slight effect on the asymmetry of the quantum plasma response. However, it is evident that an increase in both the plasma number density and the ion atomic number leads to a significant change in the plasma wave excitation resonance strength and sharpness. It is worth comparing the resonance frequency of about $\omega \simeq \pm 1$ to the one reported by Plagemann *et al.* [21] for the response of WDM with the electron number density of order 10^{23} cm^{-3}.

On the other hand, using the sum rule and integrating over the full spectrum, it is possible to calculate the static ion-structure factor (SISF) from the DISF. The result is

$$\frac{S(k)}{S_{0k}} = \int_{-\infty}^{+\infty} S_\omega(k)d\omega. \tag{13}$$

The pair correlation function (PCF), $g(r)$, which provides information on density distribution in real space, is related to SISF as

$$S(k) = 1 + n\int [g(r) - 1]\exp(i\mathbf{k}\cdot\mathbf{r})d\mathbf{r}. \tag{14}$$

In a crude approximation for dilute plasmas, the ion PCF is related to the interionic potential, $\phi_i(r)$ through $g(r) \simeq \exp[e\phi_i(r)/\kappa T_i]$. Hence, it is evident that the presence of well-defined peaks in the SISF is an indication of strong correlations among ions and their structural ordering in a quantum plasma. Figure 6 exhibits the scattering profile for different plasma fractional parameter variations. Comparing different plots in Fig. 6, we find that ion correlations are strengthened by an increase or decrease in the plasma number density or ion atomic number (compare the left and right columns in this figure). It is further observed from this figure that there is a lower electron density value where ion agglomeration and ion ordering starts to appear. For a plasma number density lower than that of solid density ($n_e \simeq 6 \times 10^{20}$ cm^{-3}) there is no indication of ion correlations [e.g., see Fig. 6(b)], while for (compressed beryllium) density of $n_e \simeq 7.4 \times 10^{25}$ cm^{-3} strong SISF peaks indicate a higher degree of long-range ion correlations. Thus, there appears to be a rule in that an increase of the plasma number density or ion atomic number might lead to sharpening or weakening of the scattering intensity pattern in the SISF of a collisional quantum plasma. This clarifies an important fact that although the ion coupling parameter is directly proportional to the ion atomic number, it cannot be a good measure for ion correlations or liquid-solid phase transitions due to the complex nature of the quantum plasma charge screening that has been reported by Shukla and Eliasson [43,50] and Akbari-Moghanjoughi [57].

Figure 7 reveals the fundamental effect of the quantum electron wave function dispersion (*viz.* tunneling of electrons through the Bohm potential), which leads to the Shukla-Eliasson attractive potential between ions, on the SISF of a quantum plasma. It is clearly confirmed that in the presence of the quantum electron wave function dispersion effect fine fringes appear in the structure of ions, which are indicative of the fact that the quantum electron wave function interference leads to stronger correlations among the plasma ions, a feature which is absent in classical plasmas. Figure 6(d) clearly shows that such a detailed correlation pattern starts at expected solid density of $n_e \simeq 10^{22}$ cm^{-3}, where the quantum electron recoil effect becomes dominant.

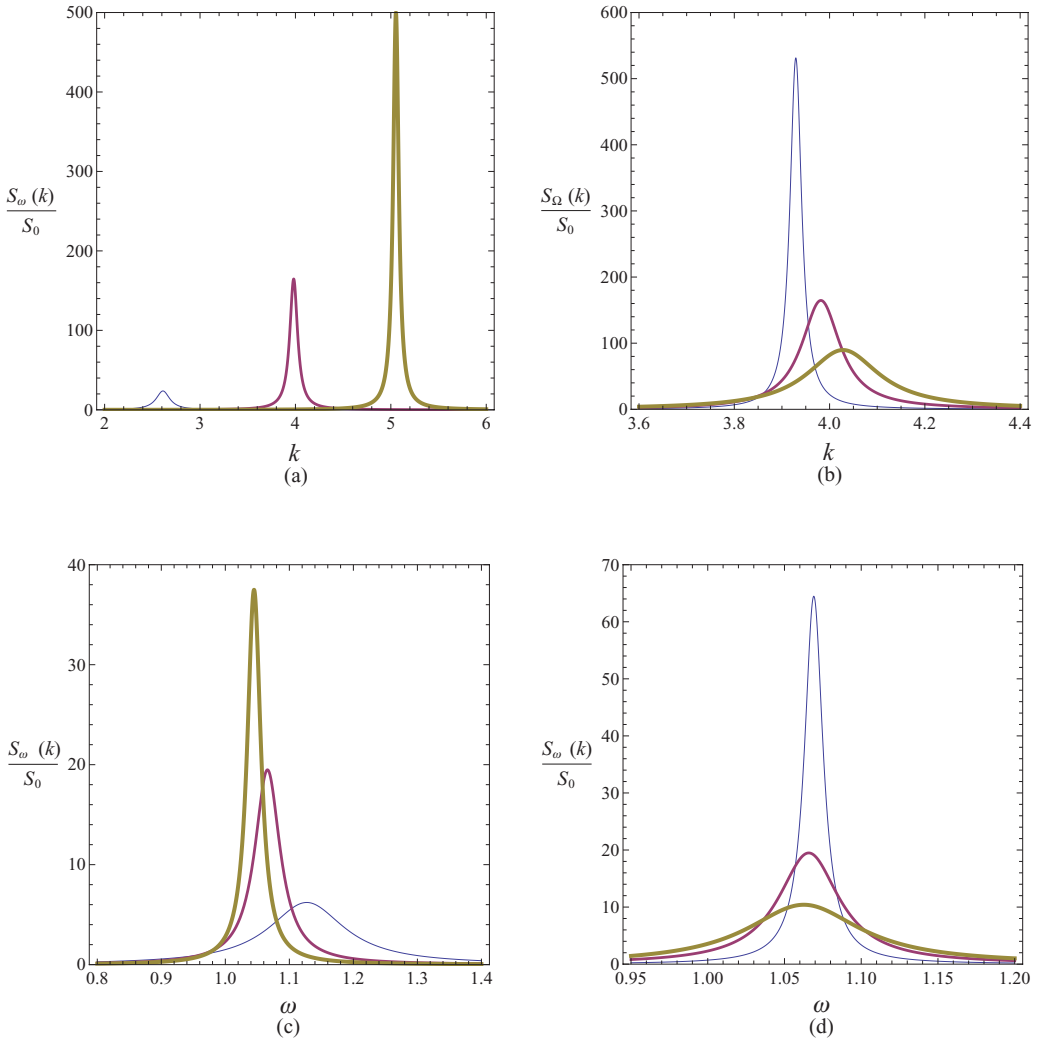

FIG. 4. (Color online) Plots of the dynamic ion structure factor for collisional quantum plasma against different plasma parameters, while one is varied and others kept fixed in each plots. The corresponding data for plots are (a) $Z_i = 2$, $n_0 = (0.47,3.8,12.7) \times 10^{25}$ cm^{-3}, $\omega = 2$, $T_i = 10^4$ K, (b) $Z_i = 1,2,3$, $n_0 = 3.8 \times 10^{25}$ cm^{-3}, $\omega = 2$, $T_i = 10^4$ K, (c) $Z_i = 2$, $n_0 = (0.47,3.8,12.7) \times 10^{25}$ cm^{-3}, $k = 1$, $T_i = 10^4$ K, and (d) $Z_i = 1,2,3$, $n_0 = 3.8 \times 10^{25}$ cm^{-3}, $k = 1$, $T_i = 10^4$ K. The increase in thickness of curves in each plots indicates the increase in the varied parameter.

IV. THE ION STOPPING POWER

The problem of energy loss has the most prominent application in ion-beam-induced inertial confinement fusion (ICF) in dense solid targets. The current scheme for ICF programs requires a detailed and accurate study of the energy-loss process for a wider density and plasma composition, which includes all the quantum interaction effects. Basic treatment of the problem, in terms of the equilibrium polarization or dielectric function, is based on the scattering rate, $Sr(k,\omega) = (4\pi Z_i e^2/k^2)^2(2\pi/\hbar^2)S_\omega(k)$. The energy-loss rate, for energy and momentum transfers, $\hbar\omega = E(p') - E(p)$ and $\hbar k = p' - p$, is then given as

$$\frac{dE}{dt} = \int \frac{Sr(k,\omega)}{2\pi\hbar}\hbar\omega d^3p = \left(\frac{Z_i e}{\pi}\right)^2 \int \frac{\omega N(\omega)}{k^2}\mathrm{Im}\left[\frac{-1}{\varepsilon(k,\omega)}\right]d^3k. \quad (15)$$

Note that range of the integral is over both negative (loss processes) and positive (gain processes) frequencies. Use of the properties of distribution function, $N(-\omega) + N(\omega) = 1$, and the dielectric function, $\varepsilon(k,-\omega) = \varepsilon^*(k,\omega)$, leads to a simplified expression for the stopping power, $S_p = -dE/dl = -(1/V_p)dE/dt$, where V_p is the projectile ion speed.

Let us now present a brief study of the ion stopping power ($S_p = -dE/dl$) and the effects of plasma parameters on the energy loss of an ion projectile in the generalized collisional quantum plasmas. The ion stopping power can provide useful information on interactions between an ion beam and dense quantum plasmas. The basic theory for the stopping power has been developed by Fermi and Teller [58]. However, since then, there has been an extensive amount of research and development on the study of stopping power of a projectile in dense degenerate plasmas [59–63]. In terms of equilibrium dielectric function, the ion stopping power can be written

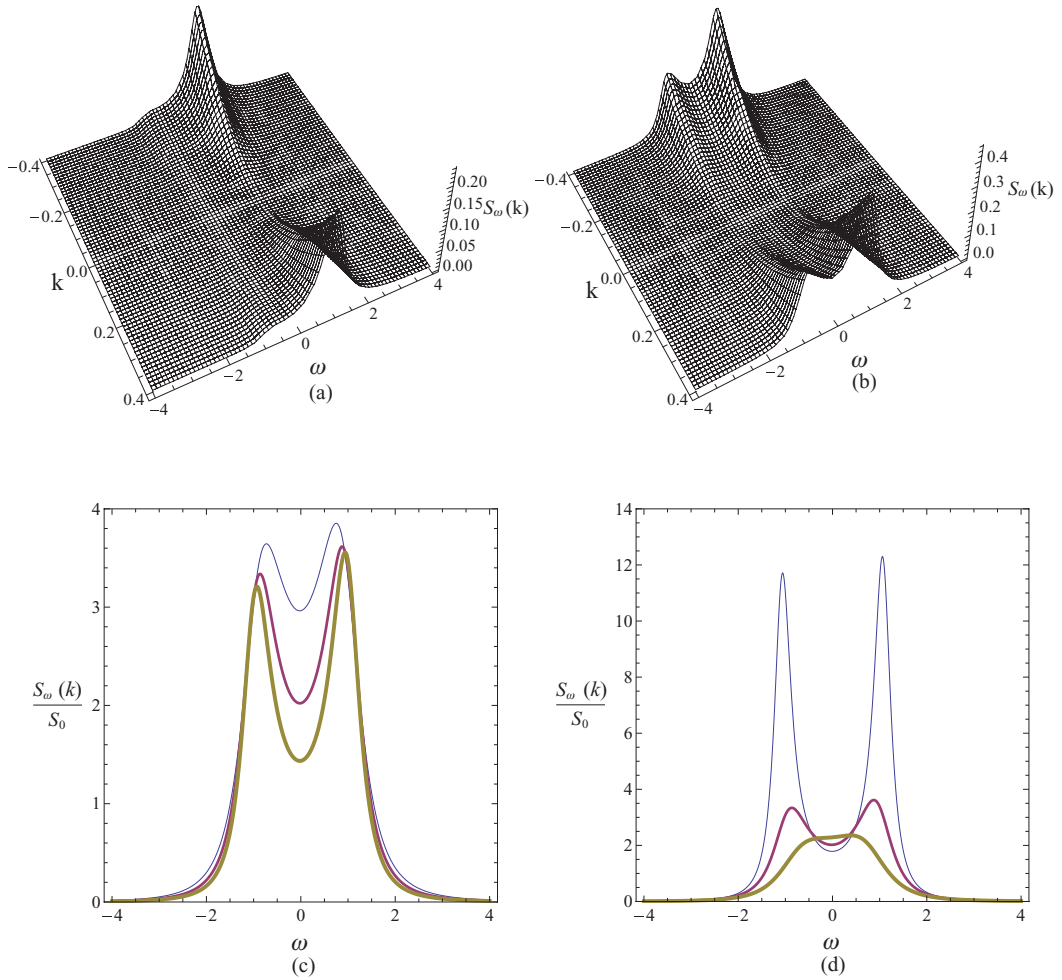

FIG. 5. (Color online) Asymmetry in plasma frequency response due to a detailed balance effect in degenerate electron fluid. The dynamic collective x-ray scattering in our viscous quantum plasma and its energy variations against different plasma parameters. The corresponding data for plots are (a) $Z_i = 6$, $R_0 = 0.02$, $T_i = 5 \times 10^4$ K, (b) $Z_i = 6$, $R_0 = 0.02$, and $T_i = 20 \times 10^4$ K (c) $Z_i = 3$, $n_0 = (2,3,4.3) \times 10^{23}$ cm^{-3}, $\lambda = 1$ Å, $T_e = 10.3$ eV, and (d) $Z_i = 1,2,3$, $n_0 = 3 \times 10^{23}$ cm^{-3}, $\lambda = 1$ Å, $T_e = 10.3$ eV. The increase in thickness of curves in each plots indicates the increase in the varied parameter.

as [64]

$$\frac{S_p(v_p,Z_i,Z_p,n)}{S_{0p}} = -\frac{Z_p^2}{v_p^2}\int_0^\infty \frac{dk}{k}\int_0^{kv_p} \mathrm{Im}[\varepsilon^{-1}(\omega,k)]\omega\, d\omega, \tag{16}$$

where Z_p is the projectile charge state and v_p is the normalized (by ω_{pe}/k_b, with $k_b = 2\pi/r_B$) projectile speed. In quantum plasmas, with free-electron fluid and static ions, the dynamic dielectric function, $\varepsilon(k,\omega)$, in the random phase approximation (RPA) has been calculated by Lindhard for arbitrary electron degeneracy, which is expressed as

$$\varepsilon_{\mathrm{RPA}}(k,\omega) = 1 + \frac{1}{\pi z^3 k_{Fe}}[g(u+z) - g(u-z)],$$
$$g(x) = \int_0^\infty \frac{y\, dy}{\exp(\beta E_{Fe} y^2 - \beta\mu) + 1} \ln\left(\frac{x+y}{x-y}\right), \tag{17}$$

where E_{Fe}, k_{Fe}, and μ are the Fermi energy, momentum, and chemical potential, respectively, and $\beta = 1/\kappa T_e$, $u = \omega/kv_{\mathrm{Fe}}$, and $z = k/2k_{\mathrm{Fe}}$. The divergence of the Lindhard dielectric function at $z = 0$ ($k = 2k_{\mathrm{Fe}}$) for a zero-temperature Fermi electron-gas model is known to lead the Freidel oscillation [65], due to discontinuity of density of states (DOS) at the Fermi surface. It is well known that the RPA approximation does not provide sufficiently accurate results for coupled plasmas with electron-ion and electron-electron interaction effects [66]. It has been recently shown that [43,50] the electron exchange-correlation effects in combination with the quantum recoil phenomenon can lead to significant modification of charge screening in quantum plasmaa and ion attractive correlations via modification of the static dielectric function. Singwi *et al.* [49,67,68] have extended the RPA dielectric function to include also the electron correlation effects. Another generalization [69] includes the effect of fluctuation in order to remove the nonanaliticity of the Lindhard dielectric function at $k = 2k_{\mathrm{Fe}}$ by taking into account the short-range electron-impurity scattering effects. Our unique hydrodynamic theory, based on fluctuation-dissipation approximation, besides the electron exchange and correlation effects, takes into account the important ionic Coulomb attractions, viscosity, and electron-ion collision effects and extends the previous investigation to relativistically degenerate density regimes

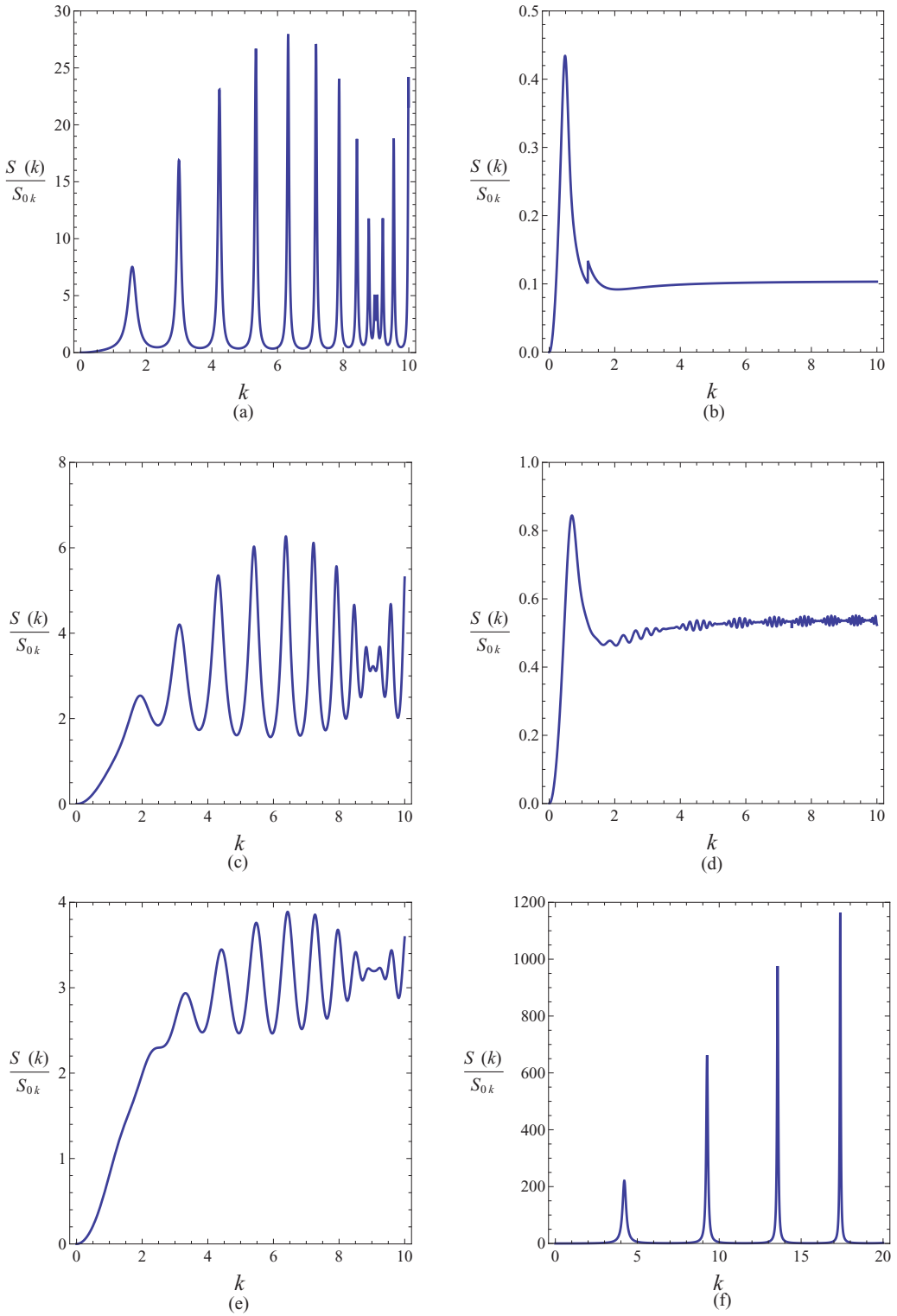

FIG. 6. (Color online) Static ion structure factors (which are related to the beam scattering intensity) and the effect of different plasma parameters on the ion correlation patterns, while only one plasma parameter is varied in each plot and others are fixed, Z_i for the first column and n_0 for the second one. The position and sharpness of peaks in each plot is related to the inverse of quasi-lattice spacing and strength of ion correlations, respectively. The corresponding data for plots are (a) $Z_i = 2$, $n_0 = 5.9 \times 10^{23}$ cm^{-3}, $T_i = 5 \times 10^3$ K, (b) $Z_i = 4$, $n_0 = 5.9 \times 10^{20}$ cm^{-3}, $T_i = 10^4$ K, (c) $Z_i = 6$, $n_0 = 5.9 \times 10^{23}$ cm^{-3}, $T_i = 5 \times 10^3$ K, (d) $Z_i = 4$, $n_0 = 1.6 \times 10^{22}$ cm^{-3}, $T_i = 10^4$ K, (e) $Z_i = 10$, $n_0 = 5.9 \times 10^{23}$ cm^{-3}, $T_i = 5 \times 10^3$ K, and (f) $Z_i = 4$, $n_0 = 7.4 \times 10^{25}$ cm^{-3}, $T_i = 10^4$ K.

beyond the existing theories. It is also observed that the generalized dielectric function, obtained here, is analytical for all wave numbers and frequencies. Current theory can provide valuable information on the fusion cross section in superdense plasmas such as those encountered in compact stellar cores and neutron star crusts.

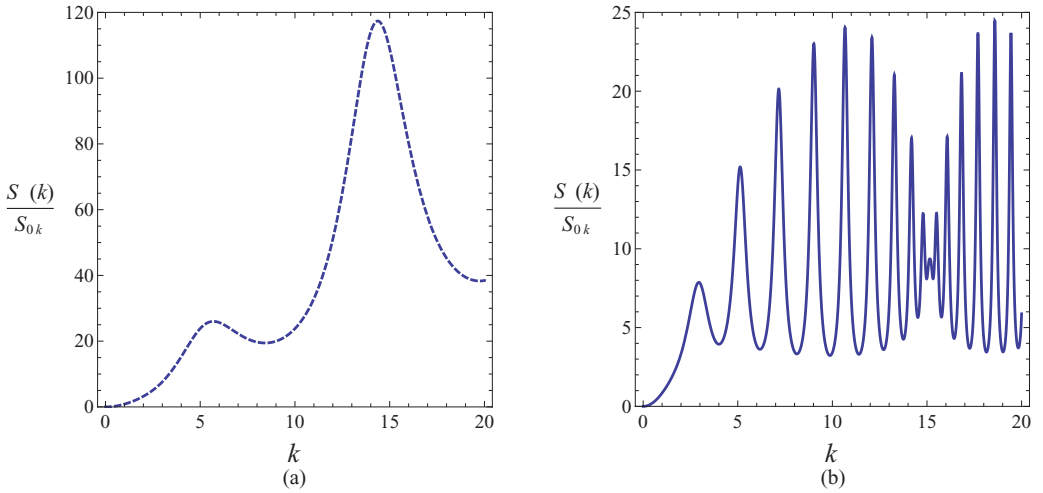

FIG. 7. (Color online) The effect of the quantum electron wave function dispersion (due to the Bohm potential, V_B) on the static ion structure factor of a collisional quantum plasma. Plots (a) and (b) correspond to static ion structure factor without and with the Bohm potential effect, respectively. Other data used for both plots are $Z_i = 10$, $n_0 = 4.7 \times 10^{24}$ cm^{-3}, $T_i = 5 \times 10^3$ K.

In current hydrodynamic quantum plasma model, the ion stopping process can be due to both collective and individual interactions among plasma species. The two most important mechanisms are the ion dragging due to the dynamic charge screening and the wake potential, which are collective phenomena, ruled by delicate interplay between electron exchange correlation, quantum statistical pressure, and quantum electron recoil effects leading to ion-ion correlations via the Shukla-Eliasson attractive force [43,50]. Also, the well-known phenomenon of the plasma polarization affects the ion stopping by the reverse field produced during the motion of a test ion projectile in the plasma (wake potential). In our model the electron-ion collisions and the ion-ion viscosity can play important roles, particularly in the nonrelativistic degenerate density regime, as deduced from Fig. 1. Nitta *et al.* [70], by using the simplified linear dielectric response model, have shown that the ion-wave excitations can play a significant role in the stopping power of classical two-component plasmas.

By using the generalized dielectric function, obtained in previous sections, we have numerically evaluated the ion stopping power for various quantum plasma parameters, such as the number density, plasma composition, projectile speed, and plasma ion temperature. Figure 8 displays the results of this numerical simulation. The projectile velocity for the maximum ion stopping power is observed to significantly vary with the change in different plasma parameter values. For instance, the ion stopping power is found to decrease with the increase in the plasma ion atomic number, while it is observed to increase with increase of the plasma number density [e.g., see Figs. 8(a) and 8(b)]. It is also found that the increase in the plasma ion atomic-number slightly lowers the corresponding projectile speed for the maximum stopping speed. This is also the case when the plasma number density increases. On the other hand, Fig. 8(c) reveals that the ion stopping power in a quantum plasma is slightly decreased by the increase of the ion temperature. Figure 8(d) further reveals that the ion stopping power increases drastically by the increase in the projectile charge state, Z_p.

V. SUMMARY AND CONCLUSIONS

In this paper, we have presented a theory for the dynamical ion structure factor (DISF) and ion stopping power (ISP) in a dense quantum plasma composed of mildly coupled degenerate electron fluids and strongly coupled nondegenerate ion fluids. Thus, we have used the quantum electron momentum equation with appropriate electrostatic and quantum forces (*viz.* associated with the quantum statistical pressure mimicking electron degeneracy, electron-exchange and electron correlation effects, and the quantum recoil effect arising from entanglements of electron wave functions over atomic scales), as well as the viscoelastic ion momentum equation including the ion correlation decay rate and the ion fluid viscosity effect. The momentum equations, which are closed with the continuity and Poisson equations, are then used to derive an expression for the dielectric constant of the collisional quantum plasma. The real and imaginary parts of the dielectric constant reveal the frequency spectra that are significantly affected by the quantum recoil effect and that play a decisive role in the description of the DISF and ISP. Our numerical results for the latter reveal that the ion coupling parameter, Γ_i, alone is not a good parameter for measuring ion correlations (as is usually assumed in the literature), but the effects of the plasma composition, the ion temperature and the average electron number density on ion correlations must be evaluated separately in our collisional quantum plasma. Specifically, our investigation of the DISF reveals long-range ion correlations due to the quantum recoil effect. Furthermore, ISP illustrates the important effects of quantum electron properties and collective ion plasma oscillations within the framework of our two-fluid approach. It is expected that ISP should play a very important role for ion energy loss in ICF and in WDM. In conclusion, we stress that the present investigation

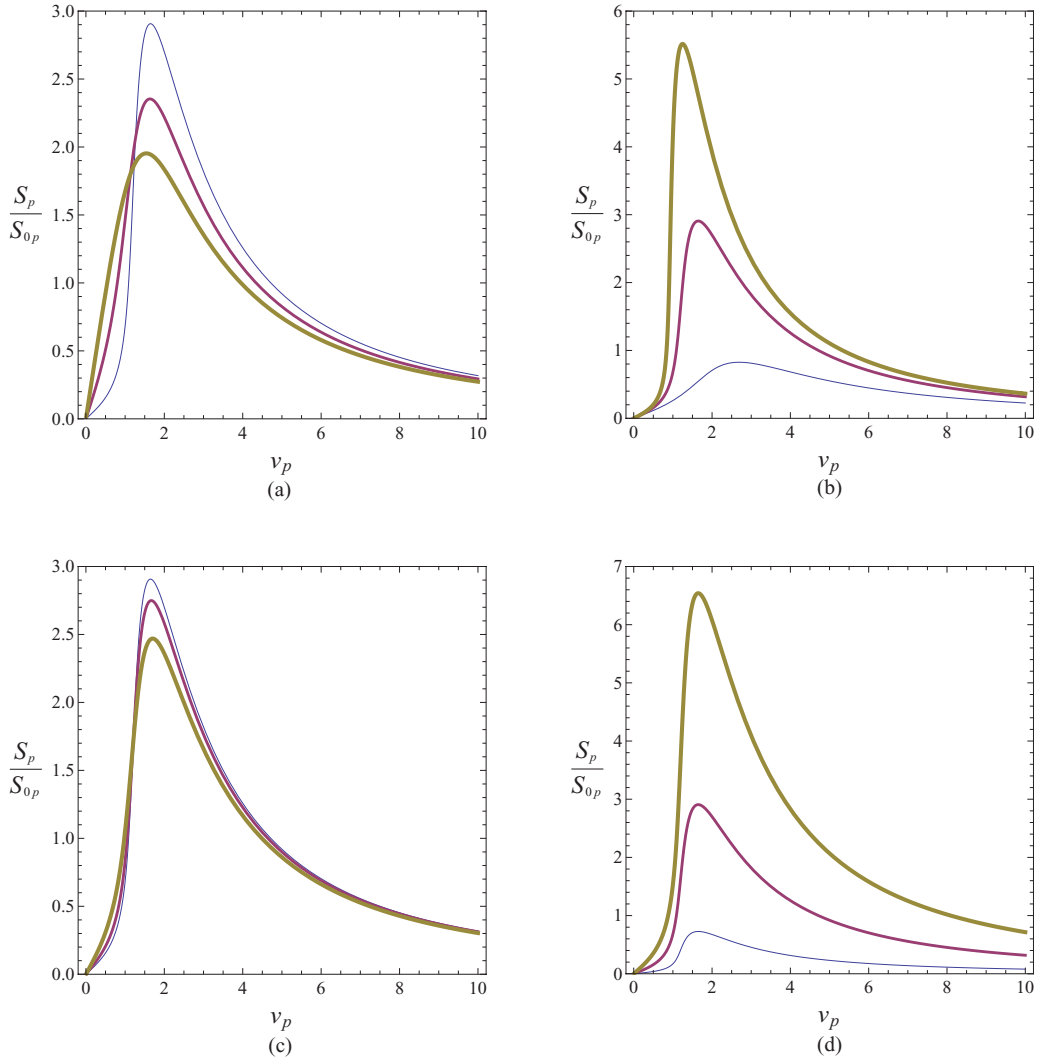

FIG. 8. (Color online) The profiles for the ion stopping power for varied ion projectile speed (the maximum stopping speeds are shown by maximum values in each plot) in terms of different plasma parameters in a nonrelativistic-degenerate density regime of viscous quantum plasma. Only one parameter is varied in each plot with the changes indicated by the change in the thickness of the curve in each plot. The corresponding data for plots are (a) $Z_i = 2,4,6$, $Z_p = 2$, $n_0 = 5.9 \times 10^{23}$ cm^{-3}, $T_i = 5 \times 10^3$ K, (b) $Z_i = 2$, $Z_p = 2$, $n_0 = (0.74,5.9,19.9) \times 10^{23}$ cm^{-3}, $T_i = 5 \times 10^3$ K, (c) $Z_i = 6$, $Z_p = 2$, $n_0 = 5.9 \times 10^{23}$ cm^{-3}, $T_i = (5,50,500) \times 10^3$ K, and (d) $Z_i = 2$, $Z_p = 1,2,3$, $n_0 = 5.9 \times 10^{23}$ cm^{-3}, $T_i = 5 \times 10^3$ K.

of the DISF and ISP should provide valuable information on the plasma x-ray scattering cross section, which is important for pulsed-power-driven high-energy-density, Z pinches, and inertial confinement fusion techniques and provide useful insight into the spectral features of the electrostatic oscillations in high-energy-density matter and in astrophysical environments (e.g., WDM and white dwarf stars), where the electron number densities are far beyond solid density and the plasma electrons are degenerate while ions are in a strongly correlated nondegenerate state.

[1] S. Ichimaru, Rev. Mod. Phys. **54**, 1017 (1982).
[2] S. Ichimaru, H. Iyetomi, and S. Tanaka, Phys. Rep. **149**, 91 (1987).
[3] S. Ichimaru, *Statistical Physics: Condensed Plasmas* (Addison Wesley, New York, 1994).
[4] V. E. Fortov and I. T. Iakunov, *The Physics of Non-Ideal Plasmas* (World Scientific, Singapore, 1999).
[5] V. E. Fortov, Phys. Usp. **52**, 615 (2009).
[6] R. Redmer, Phys. Rep. **282**, 35 (1997); S. Eliezer, P. Norreys, J. T. Mendonça, and K. Lancaster, Phys. Plasmas **12**, 052115 (2005).
[7] M. Marklund and P. K. Shukla, Rev. Mod. Phys. **78**, 598 (2006).
[8] P. K. Shukla and B. Eliasson, Rev. Mod. Phys. **83**, 25 (2009).
[9] M. Koenig, A. Benuzzi-Mounaix, A. Ravasio, T. Vinci, N. Ozaki, S. Lepape, D. Batani, G. Huser, T. Hall, D. Hicks, A. MacKinnon, P. Patel, H. S. Park, T. Boehly, M. Borghesi,

S. Kar, and L. Romagnani, Plasma Phys. Control. Fusion **47**, B441 (2005).
[10] S. Chandrasekhar, in *An Introduction to the Study of Stellar Structure* (University of Chicago Press, Chicago, 1939), p. 392.
[11] F. Hoyle and W. A. Fowler, Astrophys. J. **132**, 565 (1960).
[12] S. Chandrasekhar, Science **226**, 4674 (1984).
[13] V. S. Belyaev and V. N. Mikhaylov, Laser Phys. **11**, 957 (2011).
[14] J. M. Lattimer and M. Prakash, Astrophys. J. **550**, 426 (2001).
[15] W. L. Slattery, G. D. Doolen, and H. E. DeWitt, Phys. Rev. A **26**, 2255 (1982).
[16] S. P. Sadykova, W. Ebeling, and I. M. Tkachenko, Eur. Phys. J. D **61**, 117 (2011).
[17] G. Chabrier, N. W. Ashcroft, and H. E. Dewitt, Nature (London) **360**, 48 (1992).
[18] J. D. Lindl, P. Amendt, R. L. Berger, S. G. Glendinning, S. H. Glenzer, S. W. Haan, R. L. Kauffman, O. L. Landen, and L. J. Suter, Phys. Plasmas **11**, 339 (2004).
[19] B. Remington, R. P. Drake, and D. Ryutov, Rev. Mod. Phys. **78**, 755 (2006).
[20] J. Vorberger, Z. Donko, I. M. Tkachenko, and D. O. Gericke, Phys. Rev. Lett. **109**, 225001 (2012).
[21] K-U. Plagemann, P. Sperling, R. Thiele, M. P. Desjarlais, C. Fortmann, T. Döppner, H. J. Lee, S. H. Glenzer, and R. Redmer, New J. Phys. **14**, 055020 (2012).
[22] S. H. Glenzer and R. Redmer, Rev. Mod. Phys. **81**, 1625 (2009).
[23] E. Garcia Saiz *et al.*, Nat. Phys. **4**, 940 (2008).
[24] B. Nagler *et al.*, Nat. Phys. **5**, 693 (2009).
[25] A. L. Kritcher *et al.*, Science **322**, 69 (2008).
[26] T. Hamada and E. E. Salpeter, Astrophys. J. **134**, 683 (1961).
[27] E. E. Salpeter, Astrophys. J. **134**, 669 (1961).
[28] G. Priftis, Phys. Lett. A **27**, 577 (1968).
[29] S. H. Glenzer, O. L. Landen, P. Neumayer, R. W. Lee, K. Widmann, S. W. Pollaine, R. J. Wallace, G. Gregori, A. Höll, T. Bornath, R. Thiele, V. Schwarz, W. D. Kräeft, and R. Redmer, Phys. Rev. Lett. **98**, 065002 (2007).
[30] T. B. Mitchell, J. J. Bollinger, X.-P. Huang, and W. M. Itano, in *Trapped Charged Particles and Fundamental Physics*, edited by D. H. E. Dubin and D. Schneider, AIP Conf. Proc. 457 (AIP Press, New York, 1999), p. 309.
[31] K. Wünsch, P. Hilse, M. Schlanges, and D. O. Gericke, Phys. Rev. E **77**, 056404 (2008).
[32] Y. Klimontovich and V. P. Silin, in *Plasma Physics*, edited by J. E. Drummond (McGraw-Hill, New York, 1961), pp. 35–87.
[33] E. M. Lifshitz and L. P. Pitaevskii, *Physical Kinetics* (Buterworth-Heinemann, Oxford, 1981).
[34] G. Manfredi and F. Haas, Phys. Rev. B **64**, 075316 (2001); G. Manfredi, Fields Inst. Commun. **46**, 263 (2005); *Proceedings of the Workshop on Kinetic Theory*, The Fields Institute, Toronto, Canada, 29 March–2 April 2004.
[35] F. Haas, *Quantum Plasmas: An Hydrodynamic Approach* (Springer, New York, 2011).
[36] G. Brodin and M. Marklund, Phys. Rev. E **76**, 055403(R) (2007).
[37] G. Brodin, M. Marklund, and G. Manfredi, Phys. Rev. Lett. **100**, 175001 (2008).
[38] D. B. Melrose, *Quantum Plasmadynamics: Unmagnetized Plasmas* (Springer, New York, 2008); D. B. Melrose and A. Mushtaq, Phys. Plasmas **16**, 094508 (2009).
[39] N. Crouseilles, P. A. Hervieux, and G. Manfredi, Phys. Rev. B **78**, 155412 (2008).
[40] P. K. Shukla and B. Eliasson, Phys. Usp. **53**, 51 (2010).
[41] P. K. Shukla and B. Eliasson, Rev. Mod. Phys. **83**, 885 (2011).
[42] J. T. Mendonça, Phys. Plasmas **18**, 062101 (2011).
[43] P. K. Shukla and B. Eliasson, Phys. Rev. Lett. **108**, 219902(E) (2012); **108**, 019901(E) (2012).
[44] P. K. Shukla, Nat. Phys. **5**, 92 (2009).
[45] S. H. Glenzer, G. Gregori, R. W. Lee, F. J. Rogers, S. W. Pollaine, and O. L. Landen, Phys. Rev. Lett. **90**, 175002 (2003).
[46] G. Gregori, S. H. Glenzer, H.-K. Chung, D. H. Froula, R. W. Lee, N. B. Meezan, J. D. Moody, C. Niemann, O. L. Landen, B. Holst, R. Redmer, S. P. Regan, and H. Sawada, J. Quant. Spectrosc. Radiat. Transf. **99**, 225 (2006).
[47] H. Sagawa, S. P. Regan, D. D. Meyerhofer, I. V. Igumenshchev, V. N. Goncharov, T. R. Boehly, R. Epstein, T. C. Sangster, V. A. Smalyuk, B. Yaakobi, G. Gregori, S. H. Glenzer, and O. L. Landen, Phys. Plasmas **14**, 122703 (2007).
[48] A. Ravasio, G. Gregori, A. Benuzzi-Mounaix, J. Daligault, A. Delserieys, A. Ya. Faenov, B. Loupias, N. Ozaki, M. Rabec le Gloahec, T. A. Pikuz, D. Riley, and M. Koenig, Phys. Rev. Lett. **99**, 135006 (2007).
[49] K. S. Singwi, M. P. Tosi, R. H. Land, and A. Sejölander, Phys. Rev. **176**, 589 (1968).
[50] P. K. Shukla and B. Eliasson, J. Plasma Phys., available on CJ02012, doi: 10.1017/S0022377812001110.
[51] Frank R. Graziani *et al.*, High Energy Dens. Phys. **8**, 105 (2012).
[52] M. Akbari-Moghanjoughi and P. K. Shukla, Phys. Rev. E **86**, 066401 (2012).
[53] James P. Mithen, J. Daligault, and Gianluca Gregori, Phys. Rev. E **83**, 015401(R) (2011).
[54] P. S. Shternin, J. Phys. A **41**, 205501 (2008).
[55] D. S. Kothari and B. N. Singh, Proc. R. Soc. London, Ser. A **180**, 414 (1942).
[56] R. Nandkumar and C. J. Pethick, Mon. Not. Roy. Astron. Soc. **209**, 511 (1984).
[57] M. Akbari-Moghanjoughi, J. Plasma Phys. **79**, 189 (2013).
[58] E. Fermi and E. Teller, Phys. Rev. **72**, 399 (1947).
[59] C. K. Li and R. D. Petrasso, Phys. Rev. Lett. **70**, 3059 (1993).
[60] J. Ortner and I. M. Tkachenko, Phys. Rev. E **63**, 026403 (2001).
[61] G. Zwicknagel, C. Toepffer, and P. G. Reinhardt, Phys. Rep. **309**, 177 (1999).
[62] C. Deutsch and P. Fromy, Phys. Rev. E **61**, 4322 (2000).
[63] D. O. Gericke and M. Schlanges, Phys. Rev. E **60**, 904 (1999).
[64] J. Lindhard, K. Dan. Vidensk. Selsk. Mat. Fys. Medd. **28**, 1 (1954).
[65] D. Else, R. Kompaneets, and S. V. Vladimirov, Phys. Rev. E **82**, 026410 (2010).
[66] Manuel D. Barriga-Carrasco, Phys. Rev. E **82**, 046403 (2010).
[67] Arnold J. Glick, Phys. Rev. **129**, 1399 (1963).
[68] K. S. Singwi, M. P. Tosi, and R. H. Land, Phys. Rev. B **1**, 1044 (1970).
[69] G. Y. Hu and R. F. O'Connell, Phys. Rev. B **40**, 3600 (1989).
[70] H. Nitta, C. Muroki, and M. Nambu, Phys. Rev. E **66**, 027401 (2002).